

Fractal bodies invisible in 2 and 3 directions

Alexander Plakhov* Vera Roshchina†

Abstract

We study the problem of invisibility for bodies with a mirror surface in the framework of geometrical optics. We show that for any two given directions it is possible to construct a two-dimensional fractal body invisible in these directions. Moreover, there exists a three-dimensional fractal body invisible in three orthogonal directions. The work continues the previous study in [1, 10], where two-dimensional bodies invisible in one direction and three-dimensional bodies invisible in one and two orthogonal directions were constructed.

Mathematics subject classifications: 37D50, 49Q10

Key words and phrases: Billiards, invisible bodies, shape optimization, geometrical optics, problems of minimal resistance.

1 Introduction

Invisibility has fascinated people’s imagination since ancient times: the idea is exploited in folklore, fiction and movies. This “magical” concept is, however, rapidly migrating into the scientific domain. On the cutting edge of the modern developments is the design of metamaterials with special refractive properties, which could, amongst other important applications, ultimately lead to the creation of a real invisible cloak. For an overview of the recent works in this field we refer the reader to our recent article [10]. The aforementioned developments deal with the wave nature of light, and metamaterials are engineered at the nanoscale level. The effects specific to geometrical optics, however, also remain important in modern technology, mostly in cases where the objects are large enough for geometrical optics to dominate the wave effects. Examples include fiber optics, design of lenses (e.g. for photography or DVD readers), and many others.

In this article we are concerned with invisibility in billiards. We consider bodies with a perfectly mirrored surface in a beam of light, or, equivalently, in a flow of non-interacting

*Department of Mathematics, University of Aveiro, Aveiro 3810-193, Portugal

†CIMA, University of Évora, Portugal; Ciência 2008

billiard particles. Invisibility in a direction v (where v is a unit vector) means that any light ray which initially moves along a straight line in this direction, after several reflections from the body's surface will eventually move along the same straight line. Invisibility in a set of directions means that the above is true for any direction from this set. This problem is closely related to the problem of minimal resistance going back to Newton [7]. The latter consists of finding a body, from a given class of bodies, that experiences the smallest possible force of flow pressure, or resistance force. Since the 1990s, many interesting results on this problem have been obtained by various authors (see, e.g., [2, 3, 4, 5, 6, 8, 9]). Bodies of zero resistance in one and two directions are described in [1] and [10] respectively. In both cases it is possible to construct an invisible body by arranging several such bodies together in a specific way. In [10] it was shown that there exist bodies invisible in two mutually orthogonal directions in the three-dimensional setting and that bodies invisible in all directions do not exist.

In this work we continue the study of invisibility and construct bodies invisible in any two directions in two-dimensional space and in three orthogonal directions in three dimensions. Each body in the construction is a union of infinitely many pieces of varying size going to zero, where each piece is a domain with a piecewise smooth boundary. By slightly abusing the terminology, such a union will be called a *fractal body*, or a *solid fractal body*. In a preliminary construction (Section 3.1) and in a limiting case of the basic construction (Section 4) some pieces comprising the body are smooth curves (in the 2D case) or pieces of surfaces (in the 3D case). The corresponding body will be called a *thin fractal body*.

The article is organized as follows: we first reintroduce some definitions and briefly revisit earlier results in Section 2. In Sections 3 and 4 we explain the construction of bodies invisible in two and three directions respectively. Section 5 contains some final remarks and a brief discussion of open problems.

2 Bodies of zero resistance and invisible bodies

Consider a parallel flow of point particles in \mathbb{R}^n moving with unit velocity $v \in S^{n-1}$ towards a body B at rest. The flow is so rarefied that the particles do not mutually interact. Particles reflect elastically when colliding with the body's surface and move freely between consecutive collisions.

We deal with bounded (not necessarily connected) bodies composed of a (possibly infinite) number of piecewise smooth fragments. When a particle moving along a straight line and with a constant velocity hits the boundary of B , it is reflected from the latter without loss of speed, and keeps moving along the new linear trajectory until the next collision. All reflections are specular: the angle of incidence just before the collision is equal to the angle of reflection just after the collision (see Fig. 1). In general, it is possible that the particle never leaves the body and keeps bouncing off its sides infinitely; however,

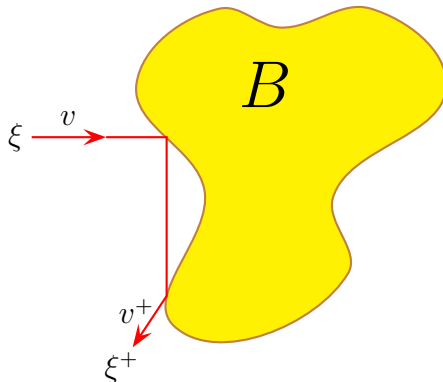


Figure 1: The broken line through the points ξ and ξ^+ is a billiard trajectory in the complement of B .

we only consider such bodies and velocities of incidence v for which almost every particle makes a finite number of reflections. Also note that in some cases the particle may hit a singular point of the boundary. In this case the further movement of the particle is not defined. We consider such bodies and velocities v that the set of initial points ξ for which the motion is undefined (i.e. such that a particle starting the movement at a point ξ in the direction v , eventually hits a singular point) has zero measure.

In view of this description, for almost any $\xi \in \mathbb{R}^n$, the particle that initially moves freely according to $x(t) = \xi + vt$, after a finite number of reflections from B moves freely again according to $x(t) = \xi^+ + v^+t$, where $\xi^+ = \xi_{B,v}^+(\xi)$ and $v^+ = v_{B,v}^+(\xi)$ are measurable functions defined almost everywhere.

Definition 1. Let a body $B \subset \mathbb{R}^n$.

- (i) We say that B has zero resistance in the direction v , if $v_{B,v}^+(\xi) = v$ for all ξ in the domain of $v_{B,v}^+$ (see Fig. 2(a)).
- (ii) We say that the body B is invisible in the direction v , if it has zero resistance in this direction and, additionally, $\xi_{B,v}^+(\xi) - \xi$ is always parallel to v (see Fig. 2(b)).
- (iii) Let $A \subset S^{n-1}$. The body B is said to be invisible/have zero resistance in the set of directions A , if it is invisible/has zero resistance in any direction $v \in A$.

Observe that invisibility is a symmetric notion, i.e. if a body is invisible in a direction v , it is also invisible in $-v$. This follows directly from the fact that billiard dynamics is time-reversible.

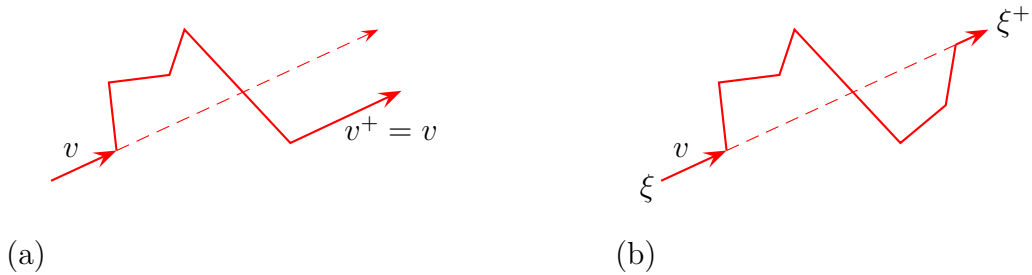


Figure 2: A typical billiard path in the case of a body (a) having zero resistance in the direction v ; (b) invisible in the direction v . The body is not shown in both cases.

Examples of bodies invisible in one direction constructed with the use of thin mirrors can be found on the Wikipedia page on invisibility [11], and one of them is reproduced in Fig. 3 (a). The German Wikipedia page [12] has got more interesting examples and

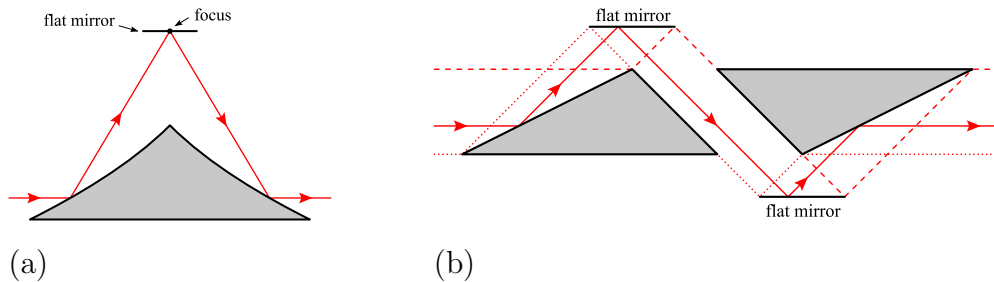


Figure 3: Bodies invisible in one direction: (a) using two parabolic mirrors and a thin flat mirror; (b) using flat mirrors.

videos of prototypes designed by Karl Bednarik (one of them that uses only flat mirrors is plotted in Fig. 3 (b)).

A solid body (i.e. without use of any thin mirrors) of zero resistance in one direction was constructed in [1] (see Fig. 4). It was also shown in the same work that there exist connected (and even homeomorphic to the ball) bodies of zero resistance in one direction. An invisible body is obtained by using two such bodies consecutively (see [1] for details).

In [10] a body of zero resistance in two directions in a three-dimensional setting was described. The body is sketched in Fig. 5: it employs 8 fragments of congruent parabolic cylinders with two mutually orthogonal focal lines (each line corresponds to 4 fragments). An invisible body is constructed by putting 4 such bodies together, as shown in Fig. 5 (b).

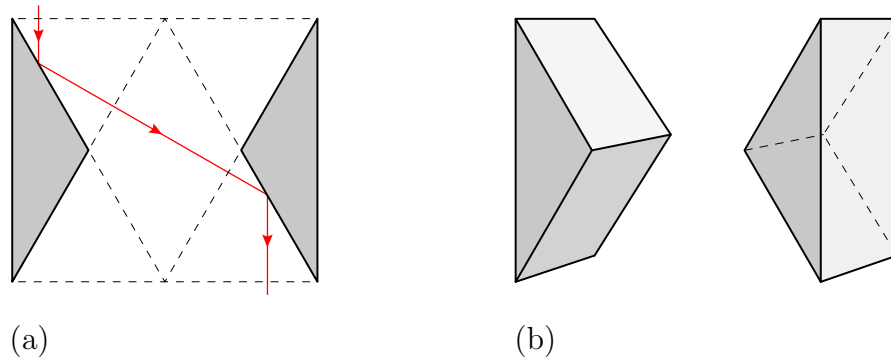


Figure 4: Solid body of zero resistance in one direction: (a) two-dimensional construction; (b) three-dimensional version.

For more details we refer the reader to [10].

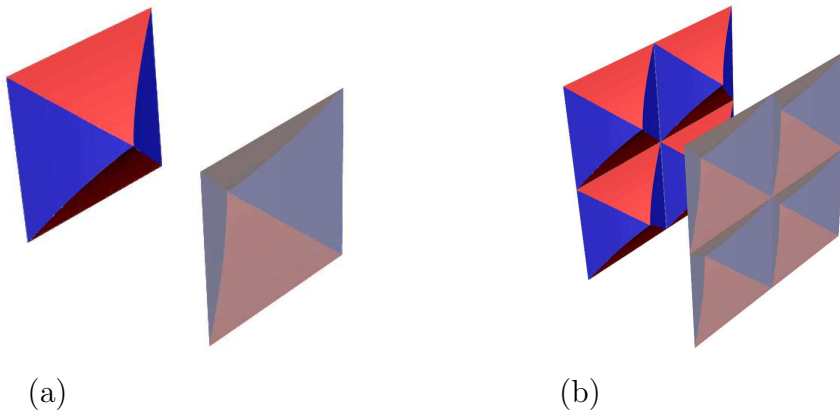


Figure 5: Solid body of zero resistance in two directions.

3 Body invisible in two directions

3.1 A thin fractal body invisible in two orthogonal directions

We start with a two-dimensional body invisible in two orthogonal directions. For the clarity of exposition, we assume that the directions of invisibility are parallel to the x - and y -axes.

We construct our body inside the square

$$S = [-1, 1] \times [-1, 1] = \{(x, y) : |x| \leq 1, |y| \leq 1\}.$$

Consider a thin parabolic mirror (i.e. having zero thickness) p_1 given by the equation

$$p_1 = \{(x, y) : y = \frac{1}{2}x^2 + \frac{1}{2}, |x| \leq 1\}.$$

Observe that $(-1, 1) \in p_1$, $(1, 1) \in p_1$, and the focus of the parabola $y = \frac{1}{2}x^2 + \frac{1}{2}$ is located at $(0, 1)$. The axis is then given by the equation $x = 0$. Also note that the mirror is located above the graph of the function $y = |x|$.

A particle moving “downwards”, i.e., along the direction $(0, -1)$, would be reflected towards the focal point due to the reflective property of a parabola (see Fig. 6 (a)).

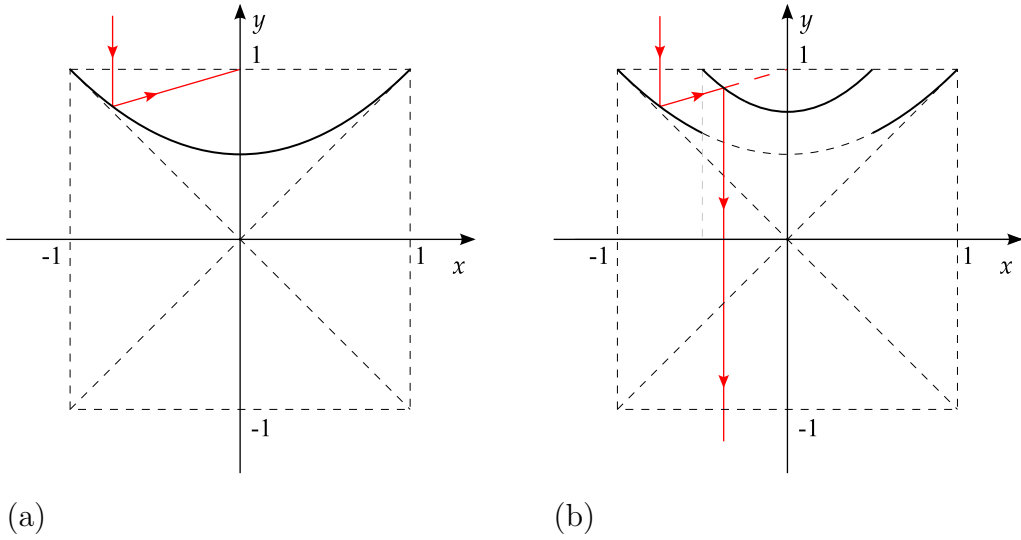


Figure 6: Fractal body invisible in two directions: (a) constructing the first parabolic mirror; (b) adding a similar confocal mirror.

We add one more parabolic mirror p_2 to our construction. This mirror is similar to the previous one, only two times smaller, while the foci of the corresponding parabolas coincide at $(0, 1)$. We let

$$p_2 = \{(x, y) : y = x^2 + \frac{3}{4}, |x| \leq \frac{1}{2}\}.$$

Now all particles that go in the downward direction and pass the line segment $[-1, -\frac{1}{2}] \times \{1\}$ (as well as $[\frac{1}{2}, 1] \times \{1\}$), are first reflected towards the focal point, move towards p_2 , and after the collision with p_2 are redirected downwards (because of the aforementioned property of a parabola and coinciding foci of the two parabolas). If we remove a piece that is directly behind p_2 from p_1 , the resulting body

$$p'_1 = \{(x, y) : y = \frac{1}{2}x^2 + \frac{1}{2}, \frac{1}{2} \leq |x| \leq 1\},$$

is not obstructing the further movement of the particles, and they leave the body with the same velocity as they had before entering the body (see Fig. 6 (b)).

If we repeat this construction process infinitely, adding figures similar to p_1 and cutting out the middle sections of the relevant parabolas, we obtain a sequence $\{p'_k\}_1^\infty$ of parabolic mirror segments:

$$p'_k = \{(x, y) : y = 2^{k-2}x^2 + 1 - 2^{-k}, 2^{-k} \leq |x| \leq 2^{-k+1}\}.$$

This mirror sequence is plotted in Fig. 7 (a). The union of these segments is denoted by $P = \cup_{k=1}^\infty p'_k$.

Take the sequence of parabolic mirror pieces q_k symmetric to p'_k with respect to the x -axis,

$$q_k = \{(x, y) : y = -2^{k-2}x^2 - 1 + 2^{-k}, 2^{-k} \leq |x| \leq 2^{-k+1}\}$$

and let $Q = \cup_{k=1}^\infty q_k$; the union $P \cup Q$ is a fractal body invisible in the direction $(0, \pm 1)$ (see Fig. 7 (b)). Indeed, since the lower part Q of our body is symmetric to the upper

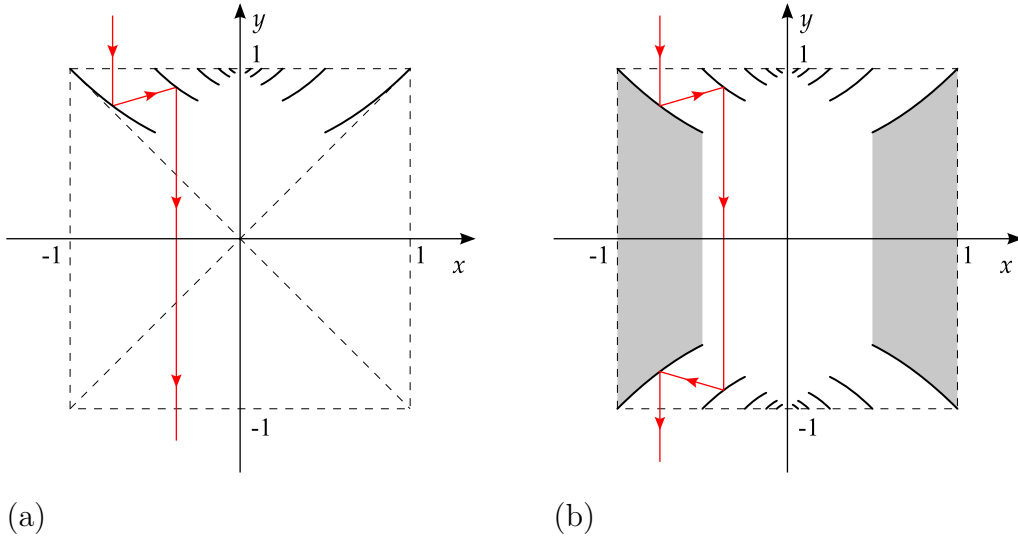


Figure 7: Fractal body invisible in two directions: (a) the basic fractal construction; (b) body invisible in the vertical direction.

part P , it is redirecting the particles back to their original trajectories.

Observe that the area

$$G = \{(x, y) : |y| \leq \frac{1}{2}x^2 + \frac{1}{2}, \frac{1}{2} \leq |x| \leq 1\}$$

(greyed in Fig. 7 (b)) is completely “shaded” from the particles moving parallel to the y -axis. We can hence use this area to make our body invisible in a second direction. We

simply add one more construction identical to the original one, but rotated by $\frac{\pi}{2}$. It is not difficult to observe that it fits into G , and also makes the body invisible in the direction $(\pm 1, 0)$. Also observe that the four grey blocks in the corners of the square (see Fig. 8), are never accessed by the particles moving in the directions of invisibility. We can hence include these areas into our body.

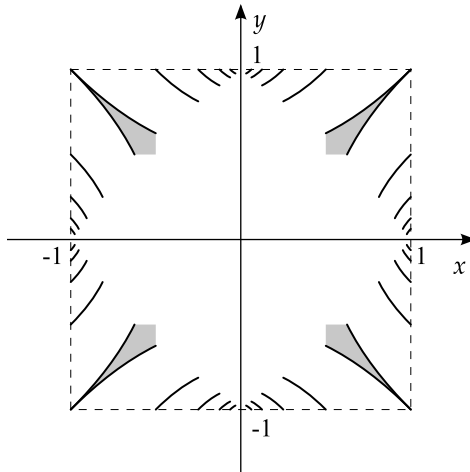


Figure 8: A thin fractal body invisible in two orthogonal directions

Thus, we have proved the following

Theorem 1. *There exists a thin fractal body invisible in two perpendicular directions.*

3.2 A body invisible in two arbitrary directions

In this section we go further and construct a two-dimensional fractal body (without thin parts) invisible in *any* two directions.

This time we construct our body inside a rhombus $ABCD$ with sides parallel to the directions of invisibility. Assume that we are given two non-parallel directions, not necessarily perpendicular. We rotate the coordinate system in a way that one of the directions is vertical. Our rhombus has got two sides parallel to the y -axis, and the other two parallel to the second direction of invisibility. The centre of the rhombus coincides with the origin.

This time our construction requires some preparatory work. Denote by $-c$ the abscissa of A and select two infinite sequences of positive values a_0, a_1, a_2, \dots and c_0, c_1, c_2, \dots recursively according to the following rules.

Let $c_0 = c$ and $a_0 = +\infty$, and choose arbitrary c_1 satisfying $0 < c_1 < c_0$. On the i th step of the procedure, $i = 1, 2, \dots$ select arbitrary a_i satisfying the inequalities

$$0 < a_i < a_{i-1} \quad \text{and} \quad a_i(c_{i-1} - 2c_i) < c_i^2 \quad (1)$$

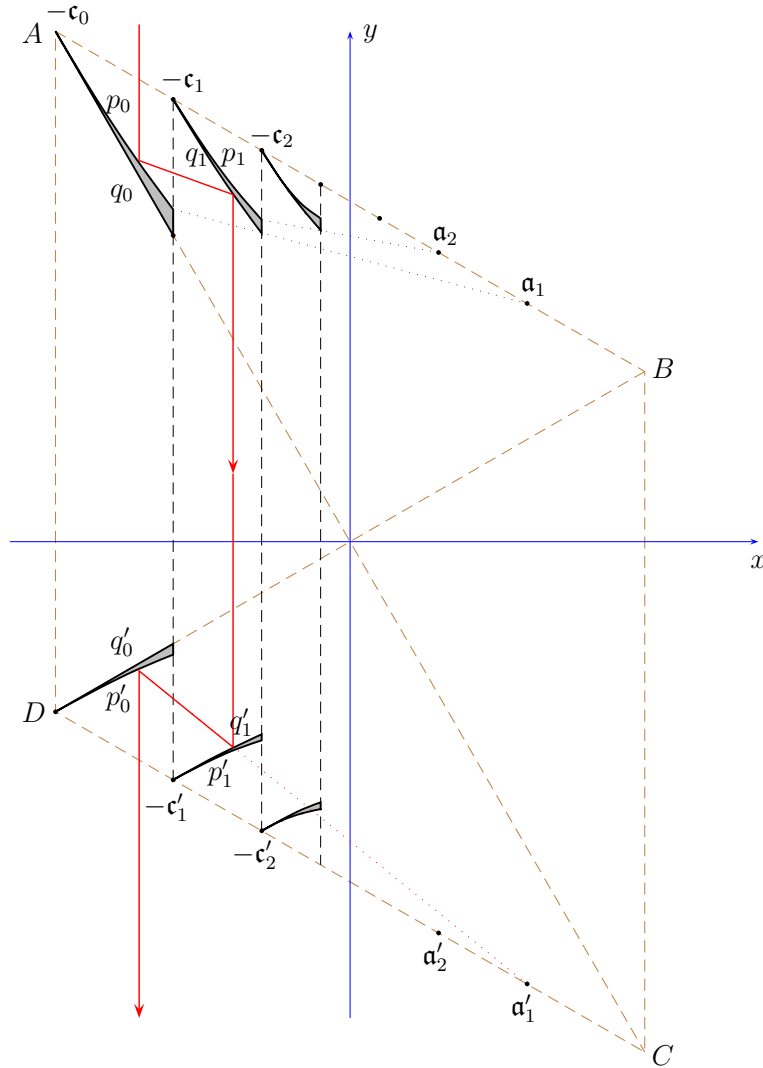


Figure 9: Preliminary construction: A body inside a rhombus invisible in one direction.

and put

$$c_{i+1} = \frac{(c_i + a_i)^2}{c_{i-1} + a_i} - a_i. \quad (2)$$

Using (1) and (2), one easily gets that $c_i > 0$ and derives by induction that $c_{i+1} < c_i$.

Now we are ready to draw the parabolas of our construction. In the description below, the points on the side AB are marked by the values of their abscissas: $-c_0, -c_1, -c_2, \dots, a_1, a_2, \dots$ (see Fig. 9).

For any $i = 0, 1, 2, \dots$ consider the parabola through $-c_i$ with a vertical axis and with the focus at a_{i+1} . Denote by p_i the arc of this parabola bounded by the points with abscissas $-c_i$ and $-c_{i+1}$. Then for any $i = 1, 2, \dots$ consider the parabola through $-c_i$ with a vertical axis and with the focus at a_i . The arc of this parabola situated between

the points with abscissas $-c_i$ and $-c_{i+1}$ is denoted by q_i . Also denote by q_0 the part of the diagonal AC between A and the point with abscissa $-c_1$. Each arc p_i is situated above q_i ; more precisely, both p_i and q_i are the graphs of functions $p_i(-t)$ and $q_i(-t)$, $t \in [c_{i+1}, c_i]$ with $p_i(-t) > q_i(-t)$ for any $t \in (c_{i+1}, c_i]$. Denote by P_i , $i = 0, 1, 2, \dots$ the set bounded by the arcs p_i and q_i from above and below and by a segment of the vertical line $x_i = -c_{i+1}$ on the right.

Similarly, denote by $-c'_i$ and a'_i , respectively, the points on the side CD whose abscissas are $-c_i$ and a_i (the same values as above). Denote by p'_i (q'_i) the arc of parabola through $-c'_i$ with vertical axis and with focus at a'_{i+1} (a'_i) bounded by the vertical lines $x = -c_i$ and $x = -c_{i+1}$. Introduce the sets P'_i bounded by p'_i , q'_i and the segment of line $x = -c_{i+1}$.

Denote by H_i ($i = 1, 2, \dots$) the homothety with the centre a_i and ratio $r_i = (c_i + a_i)/(c_{i-1} + a_i)$.

Proposition 1. *The arcs p_{i-1} and q_i are homothetic under H_i .*

Proof. Note that the parabolas containing p_{i-1} and q_i have the same focus at a_i ; therefore they are homothetic with the centre at this point. Since the points $-c_{i-1}$ and $-c_i$ (which are the left endpoints of the arcs p_{i-1} and q_i) are homothetic, one readily concludes that the ratio equals r_i , and therefore, the homothety is H_i . Further, the right endpoint of p_{i-1} has abscissa $-c_i$; using (2), one verifies that its image under H_i has the abscissa $-c_{i+1}$, and therefore, coincides with the right endpoint of q_i . Thus, the arcs p_{i-1} and q_i belong to homothetic parabolas, and their right and left endpoints are homothetic; therefore they are also homothetic under H_i . \square

Consider the fractal body (greyed in Figure 9)

$$\mathcal{A}_L = (\cup_{i=0}^{\infty} P_i) \cup (\cup_{i=0}^{\infty} P'_i).$$

Now we are in a position to prove the following Proposition.

Proposition 2. *The body \mathcal{A}_L is invisible in the vertical direction.*

Proof. Consider a particle falling vertically downward with the velocity $(0, -1)$ along a line with abscissa x . We assume that $x \in [-c, 0]$; otherwise the particle does not hit the body and there is nothing to prove. If $x = -c_i$ ($i = 0, 1, 2, \dots$), the particle hits the body at a singular point and the motion is not defined from this point. Otherwise, x belongs to an interval (c_{i-1}, c_i) , $i = 1, 2, \dots$ ($i = 1$ in Fig. 9).

The particle is first reflected by p_{i-1} and then moves to the focus a_i ; then it makes the second reflection from q_i and moves along a vertical line. Since the line through the two reflection points contains the focus, these two points (and therefore the vertical lines through these points) are homothetic under H_i .

The particle then makes the third and fourth reflections from q'_i and p'_{i-1} , and finally, moves freely downwards. Repeating the above argument, one concludes that the vertical

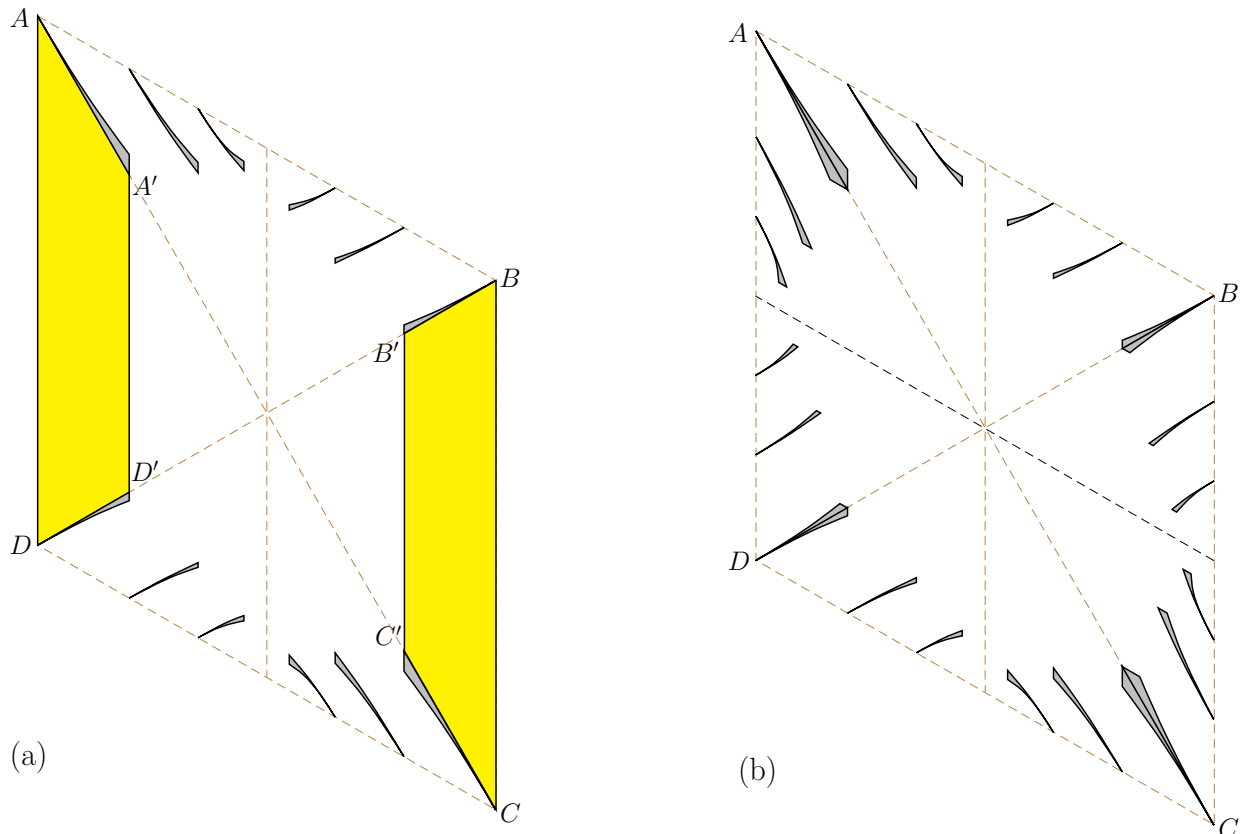


Figure 10: (a) A centrally symmetric body invisible in one direction and the shaded regions. (b) A body invisible in two directions.

lines through the third and fourth reflection points are homothetic under the inverse homothety H_i^{-1} , and therefore, the vertical lines containing the initial and final parts of the trajectory coincide. \square

By adding the set \mathcal{A}_R symmetric to \mathcal{A}_L with respect to the centre of the rhombus, one gets the body $\mathcal{A} = \mathcal{A}_L \cup \mathcal{A}_R$, which is also invisible in the vertical direction $(0, -1)$ (Fig. 10 (a)).

Remark 1. The arcs $p_i, q_i, p'_i, q'_i, i = 0, 1, 2, \dots$ are graphs of functions; denote these functions by $p_i(-x), q_i(-x), p'_i(-x), q'_i(-x), x \in [c_{i+1}, c_i]$. Then the sets P_i, P'_i can be represented as

$$P_i = \{(x, y) : -c_i \leq x \leq -c_{i+1}, q_i(-x) \leq y \leq p_i(-x)\},$$

$$P'_i = \{(x, y) : -c_i \leq x \leq -c_{i+1}, p'_i(-x) \leq y \leq q'_i(-x)\}.$$

In particular, if the directions of invisibility are orthogonal, we have $p'_i(x) = -p_i(x), q'_i(x) = -q_i(x)$, and the body \mathcal{A} is analytically described as

$$\mathcal{A} = \cup_{i=0}^{\infty} \{(x, y) : c_{i+1} \leq |x| \leq c_i, q_i(|x|) \leq |y| \leq p_i(|x|)\}.$$

This representation will be used in the next section.

Observe that the trapezoids $AA'D'D$ and $BB'C'C$ bounded by the lines $x = \pm c_0$, $x = \pm c_1$ and by the diagonals of the rhombus are completely “shaded” from the particles falling in the vertical direction. We can therefore use this area to make our body invisible in the second direction.

Namely, the body \mathcal{B} symmetric to \mathcal{A} with respect to the line BD (or AC) is contained in the union of the trapezoids and is invisible in the direction \overrightarrow{AB} . The union $\mathcal{A} \cup \mathcal{B}$ is then invisible in both directions (Fig. 10 (b)).

We have proved the following result. Observe that it includes Theorem 1 as a particular case.

Theorem 2. *For any two directions v_1 and $v_2 \in S^1$, there exists a solid fractal body invisible in these directions.*

Remark 2. *In the limiting case $c_i = 2^{-i}c$, $a_i = 0$ ($i \geq 1$) one gets a thin fractal. In particular, if the two directions are orthogonal, we have the construction described in the previous Subsection 3.1.*

4 A body invisible in 3 directions

Using the two-dimensional construction described in the previous section, we can now describe a three-dimensional body invisible in 3 orthogonal directions.

In the 3D case the construction is more complicated and intuition is less reliable; therefore we provide here a more detailed argument than in the previous section. Some of the accompanying figures, for better visibility, correspond to the limiting case of *thin* fractal body.

Let us first introduce some notation. We consider Euclidean space \mathbb{R}^3 with orthogonal coordinates x, y, z and the cube $Q = [-c, c]^3$ centered at the origin $O = (0, 0, 0)$. The pyramids with the vertex at O and with the bases $z = \pm c$, $|x| \leq c$, $|y| \leq c$ (the upper and lower faces of the cube Q) are denoted by Π_z^\pm . In other words,

$$\Pi_z^\pm = \{(x, y, z) \in Q : \pm z \geq \max\{|x|, |y|\}\}.$$

Further, $\Pi_z = \Pi_z^+ \cup \Pi_z^-$. The pyramids Π_x and Π_y are defined in the same way. Notice that the interiors of Π_x , Π_y , and Π_z are mutually disjoint.

Let $0 < c_1 < c$. For each $\varepsilon_x \in \{-1, 1\}$ and $\varepsilon_z \in \{-1, 1\}$ we define the gallery

$$G(\varepsilon_x, \varepsilon_z) = \varepsilon_x[c_1, c] \times [-c, c] \times \varepsilon_z[c_1, c]$$

(where by definition $\varepsilon[a, b] = \begin{cases} [\varepsilon a, \varepsilon b], & \text{if } \varepsilon > 0 \\ [-\varepsilon b, -\varepsilon a], & \text{if } \varepsilon < 0 \end{cases}$); it is a horizontal parallelepiped adjacent to an edge of Q parallel to the y -axis. The union of 4 such parallelepipeds is

$$G_y = \cup_{\varepsilon_x, \varepsilon_z = \pm 1} G(\varepsilon_x, \varepsilon_z).$$

The sets G_x and G_z are defined similarly.

We are going to define three bodies B_x , B_y , B_z , invisible in the directions x , y , z , respectively, and then take their union.

First we take the two-dimensional body $\mathcal{A} = \mathcal{A}_{yz}$ in the yz -plane, as described in the previous subsection 3.2. It corresponds to 2 *orthogonal* directions (parallel to the y - and z -axes) and is inscribed in the square $[-c, c]^2$. (Notice that the body \mathcal{A} shown in Fig. 10 (a) corresponds to 2 *non-orthogonal* direction and is inscribed in a rhombus.) The body \mathcal{A}_{yz} invisible in the z -direction is determined by the parameters $c_0 = c$, c_1, c_2, \dots ; a_1, a_2, \dots satisfying (1) and (2).

Take the direct product

$$\tilde{\mathcal{A}}_{yz} = ([-c, -c_1] \cup [c_1, c]) \times \mathcal{A}_{yz};$$

the resulting three-dimensional body $\tilde{\mathcal{A}}_{yz}$ is also invisible in the z -direction. Notice that it is contained in the union of y -galleries,

$$\tilde{\mathcal{A}}_{yz} \subset G_y. \quad (3)$$

The body $\tilde{\mathcal{A}}_{yz}$ is shown in Fig. 11 (a); for the sake of better visualization we chose to draw the limiting case of “thin fractal” with $a_i = 0$ and $c_i = 2^{-i}c$ ($i = 1, 2, \dots$).

Let $B_{yz} = \tilde{\mathcal{A}}_{yz} \cap \Pi_z$ (Fig. 11 (b)). Then we analogously define the body B_{xz} and take

$$B_z = B_{yz} \cup B_{xz}.$$

The bodies B_x and B_y are defined in a similar way, and finally,

$$B = B_x \cup B_y \cup B_z.$$

The bodies B_z , B_y and B_x are shown on Fig. 13 (a), Fig. 13 (b) and Fig. 14 (a) respectively. The body B is shown on Fig. 14 (b). All the pictures correspond to the “thin” fractal case.

Remark 3. *In terms of the functions p_i and q_i introduced in Remark 1, the set $\tilde{\mathcal{A}}_{yz}$ can be written as*

$$\tilde{\mathcal{A}}_{yz} = \cup_{i=0}^{\infty} \{(x, y, z) : c_{i+1} \leq |y| \leq c_i, q_i(|y|) \leq |z| \leq p_i(|y|), c_1 \leq |x| \leq c\}.$$

Taking the intersection of $\tilde{\mathcal{A}}_{yz}$ with $\Pi_z = \{(x, y, z) : |z| \geq |x|, |z| \geq |y|\}$ and using that $q_i(|y|) \geq |y|$, one gets

$$B_{yz} = \cup_{i=0}^{\infty} \{(x, y, z) : c_{i+1} \leq |y| \leq c_i, q_i(|y|) \leq |z| \leq p_i(|y|), c_1 \leq |x| \leq |z|\},$$

and therefore,

$$B_{yz} \subset \cup_{i=0}^{\infty} \{(x, y, z) : c_{i+1} \leq |y| \leq c_i, |x| \leq p_i(|y|)\}. \quad (4)$$

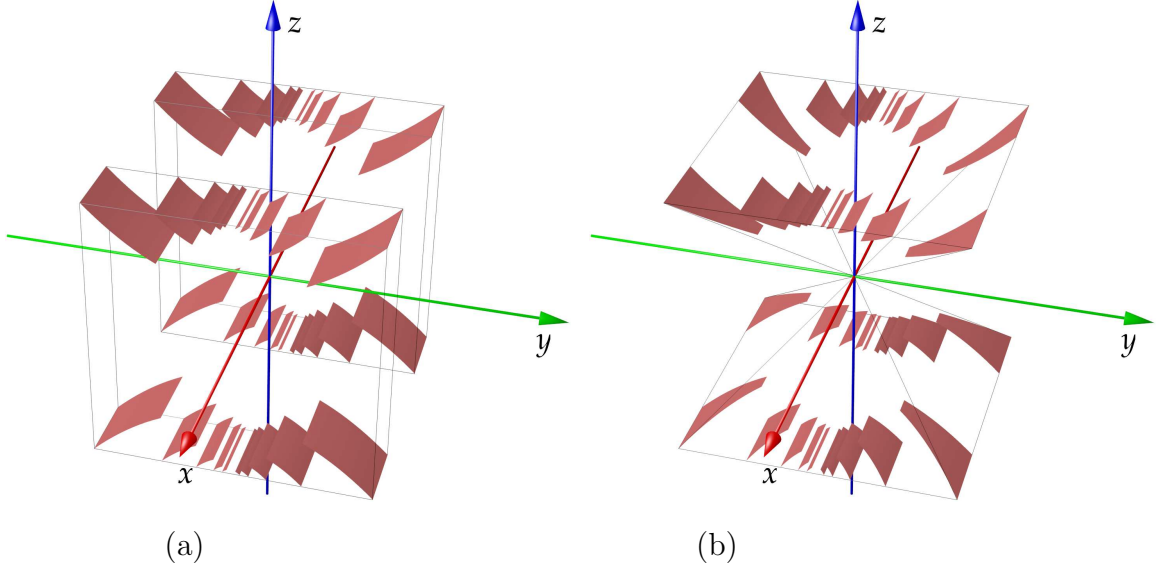


Figure 11: The bodies (a) $\tilde{\mathcal{A}}_{yz}$ and (b) B_{yz} are shown in the *thin fractal* case.

Similar relations are true for the other sets B_{yx} , B_{xz} , etc; for example,

$$B_{xz} = \cup_{i=0}^{\infty} \{(x, y, z) : c_{i+1} \leq |x| \leq c_i, q_i(|x|) \leq |z| \leq p_i(|x|), c_1 \leq |y| \leq |z| \leq c\}, \quad (5)$$

$$B_{yx} \subset \cup_{i=0}^{\infty} \{(x, y, z) : c_{i+1} \leq |y| \leq c_i, q_i(|y|) \leq |x| \leq p_i(|y|)\}. \quad (6)$$

Now we are prepared for the proof of the following theorem.

Theorem 3. *There exists a solid fractal body invisible in 3 mutually orthogonal directions.*

Proof. We are going to show that B is invisible in the directions parallel to the coordinate axes.

It suffices to prove that B is invisible in the z -direction; this will imply invisibility in the x - and y -directions, due to symmetry of the construction under the exchange of variables x , y and z . We will actually show that the body B_z is invisible for the incident flow in the z -direction and the bodies B_x and B_y are shadowed from this flow by B_z .

Consider an incident particle with the velocity $(0, 0, -1)$. Our goal is to prove that it makes either 0 or 4 reflections from B_z (and no reflections from B_x and B_y) and moves freely afterwards; moreover, the initial and final parts of its trajectory belong to the same straight line.

If the orthogonal projection of the coordinate of the incident particle on the xy -plane lies inside the square $[-c_1, c_1]^2$ or outside the square $[-c, c]^2$ (see Fig. 12), the particle does not hit the body and there is nothing to prove. It remains therefore to consider the case where the projection is contained in $[-c, c]^2 \setminus [-c_1, c_1]^2$.

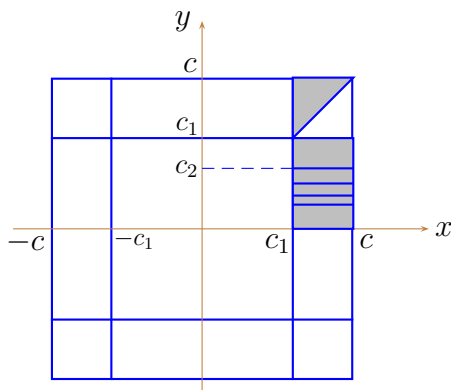


Figure 12: The frame of the construction in the xy -projection.

Due to symmetry of the construction, it suffices to consider the cases where the projection belongs to (i) the triangle $c_1 < x < y < c$ and (ii) the rectangle $c_1 < x < c$, $0 < y < c_1$ (they are shown grey in Fig. 12).

Consider the case (i). Take an auxiliary trajectory corresponding to the particle with the same initial data making reflections from $\tilde{\mathcal{A}}_{yz}$. At the first point of reflection one has $z = p_0(y)$, at the second point, $z = q_1(y)$, and the third and fourth reflection points are symmetric to the first two points with respect to the xy -plane. After the fourth reflection the particle moves freely. We know that $\tilde{\mathcal{A}}_{yz}$ is invisible in the z -direction; that is, the initial and final parts of the auxiliary trajectory belong to a straight line. It remains to show that the points of impact actually belong to B_{yz} and the auxiliary trajectory does not intersect the rest of the body $B \setminus B_{yz}$; this will imply that it is a *true* billiard trajectory in the complement of B .

The parts of the auxiliary trajectory in Q before the first reflection, between the first and the second reflection, and between the second and the third reflection will be referred to as 01-segment, 12-segment, and 23-segment, respectively. At the first reflection point $(x^{(1)}, y^{(1)}, z^{(1)})$ one has

$$z^{(1)} = p_0(y^{(1)}) > y^{(1)} > x^{(1)},$$

therefore this point belongs to the interior of Π_z , and so, $(x^{(1)}, y^{(1)}, z^{(1)}) \in B_{yz}$. At the second reflection point $(x^{(2)}, y^{(2)}, z^{(2)})$ one has $x^{(2)} = x^{(1)}$, $0 < y^{(2)} < y^{(1)}$, and $z^{(2)} > z^{(1)}$, therefore this point also belongs to the interior of Π_z , and so, $(x^{(2)}, y^{(2)}, z^{(2)}) \in B_{yz}$. Since Π_z is convex, one concludes that the segment with endpoints $(x^{(1)}, y^{(1)}, z^{(1)})$ and $(x^{(2)}, y^{(2)}, z^{(2)})$ also belongs to the interior of Π_z .

Using (5) and the inequality $c_1 < x^{(1)} < c$, one concludes that the intersection of B_{xz} with the plane $x = x^{(1)}$ belongs to the set $\{c_1 \leq |y| \leq c, z \leq p_0(x^{(1)})\}$. On the other hand, $p_0(x^{(1)}) < p_0(y^{(1)})$ and the 01- and 12-segments belong to the set $\{z \geq p_0(y^{(1)})\}$, and the 23-segment belongs to the set $\{|y| < c_1\}$. This implies that the first three segments of the trajectory do not intersect B_{xz} , and due to the symmetry of both B_{xz} and the trajectory with respect to the xy -plane, this is true for the whole trajectory.

Further, the 01- and 12-segments belong to the interior of Π_z , and therefore, do not

intersect B_x and B_y . Due to the symmetry with respect to the xy -plane, this is also true for the last two segments of the auxiliary trajectory. It remains therefore to prove that the 23-segment does not intersect the bodies $B_x = B_{yx} \cup B_{zx}$ and $B_y = B_{zy} \cup B_{xy}$.

The sets B_{zx} , B_{zy} and B_{xy} belong to the galleries G_z and G_x , and therefore cannot have points in common with the 23-segment. It remains to check the set B_{yx} .

At the second reflection point $(x^{(2)}, y^{(2)}, z^{(2)})$ one has $z^{(2)} = q_1(y^{(2)})$ and $z^{(2)} > x^{(2)}$. At each point of the 23-segment one has $x = x^{(2)}$, $y = y^{(2)}$, and therefore, $x < q_1(y)$ and $c_2 < y < c_1$. By (6), no such point belongs to B_{yx} .

Consider now the case (ii). Take $i \geq 1$ such that $c_{i+1} < y < c_i$. (The limiting case $y = c_i$ has zero measure in the space of billiard trajectories; in this case the particle hits a singular point of B and the motion is not defined since then.)

If $x > p_i(y)$, the particle does not hit B . Indeed, by (4), the vertical straight line $(x, y, *)$ does not intersect B_{yz} , and by (6), it does not intersect B_{yx} . The other sets B_{xy} , B_{xz} , B_{zx} , B_{zy} comprising B belong to the galleries G_x and G_z , and therefore do not intersect this straight line.

Assume that $x < p_i(y)$ and consider an auxiliary trajectory with the same initial data making reflections from \tilde{A}_{yz} . As in the case (i), there are 4 reflections; the first three segments of the trajectory (between the point of entering Q and the 1st reflection point; between the 1st and the 2nd reflection points; between the 2nd and the 3rd reflection points) will be referred to as 01-segment, 12-segment, and 23-segment, respectively. The trajectory is symmetric with respect to the xy -plane, and the final velocity, $(0, 0, -1)$, coincides with the initial one.

Repeating the argument of (i), one concludes that the 1st and 2nd reflection points and the 12-segment joining them belong to Π_z , and by symmetry, the 3rd and 4th reflection points, and the segment joining them, also belong to Π_z . Therefore all the reflection points belong to B_{yz} . It remains to check that the auxiliary trajectory does not intersect $B \setminus B_{yz}$, and therefore, is a *true* trajectory in the complement of B .

Recall that the sets B_{xy} , B_{xz} , B_{zx} , B_{zy} belong to $G_x \cup G_z$, and therefore do not intersect the trajectory. It remains to check the set B_{yx} . Since the 01- and the 12-segments belong to Π_z , they do not have points in common with B_{yx} . The same is true for the last two segments symmetric to them. It remains to check the 23-segment.

Let $(x^{(1)}, y^{(1)}, z^{(1)})$ and $(x^{(2)}, y^{(2)}, z^{(2)})$ be the points of first and second reflection. Notice that the 23-segment belongs to the straight line $(x^{(2)}, y^{(2)}, *)$. One has

$$c_{i+2} < y^{(2)} < c_{i+1}, \quad (7)$$

$x^{(2)} = x^{(1)} = x$, $0 < y^{(2)} < y^{(1)} = y$, $p_i(y^{(1)}) < q_{i+1}(y^{(2)})$, and therefore,

$$x^{(2)} < q_{i+1}(y^{(2)}). \quad (8)$$

By (6),(7), and (8), the straight line $(x^{(2)}, y^{(2)}, *)$ does not intersect B_{yx} . Hence the theorem is proved. \square

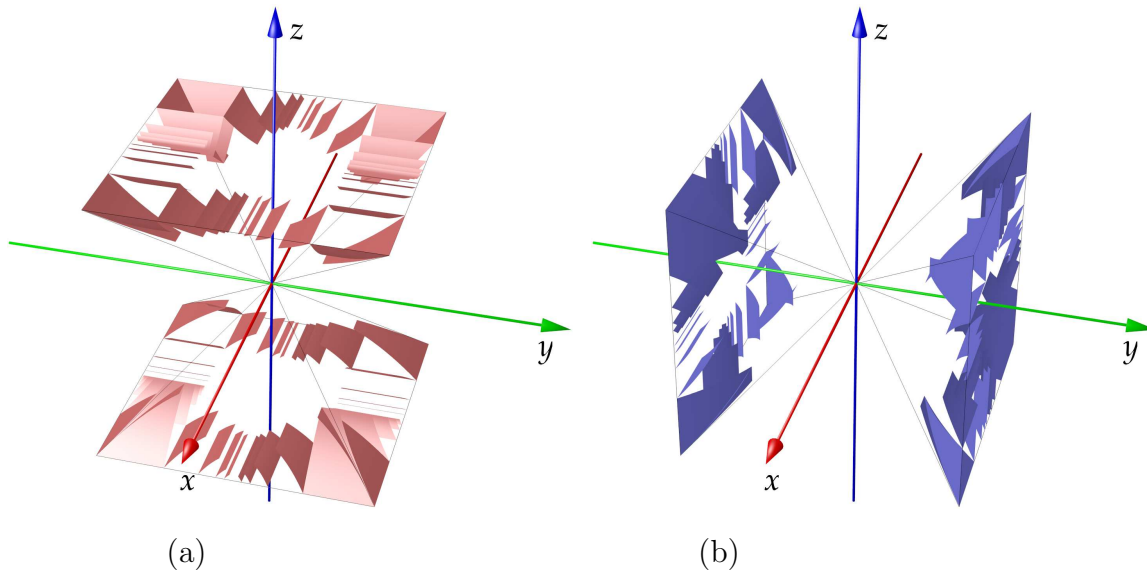


Figure 13: Non-overlapping bodies invisible in different directions: (a) along the z -axis; (b) along the y -axis

Remark 4. *We do not know if it is possible to generalize our construction to 3 non-orthogonal directions. The direct generalization does not work even in the case where two non-orthogonal directions lie in the xy -plane and the third one coincides with the z -direction. Indeed, a particle falling vertically down and hitting a mirror in the gallery G_y , will then move in a direction orthogonal to the y -axis (and not parallel to the x -axis, which would be desirable), and therefore may fail to hit the opposite mirror in that gallery.*

5 Summary

We have shown that there exist bodies invisible in 2 directions in the two-dimensional case and in 3 directions in the three-dimensional case. It was not known earlier whether such bodies exist. We believe that our construction can be more or less directly generalized to n directions of invisibility for n -dimensional bodies, $n > 3$.

There are, however, many open questions. Can we construct a body invisible in n directions in n -dimensional space without using any fractal constructions? Are there bodies invisible in more than n directions in n -dimensional space? What is the maximal number of directions of invisibility? How to introduce an adequate “measure of invisibility” for a body observed in all directions and find the “most invisible” body?

There is an intriguing observation related to the existing constructions. There exist connected (and even homeomorphic to the ball) bodies invisible in 1 direction [1]. The body invisible in 2 directions found in [10] is disconnected. The body invisible in 3

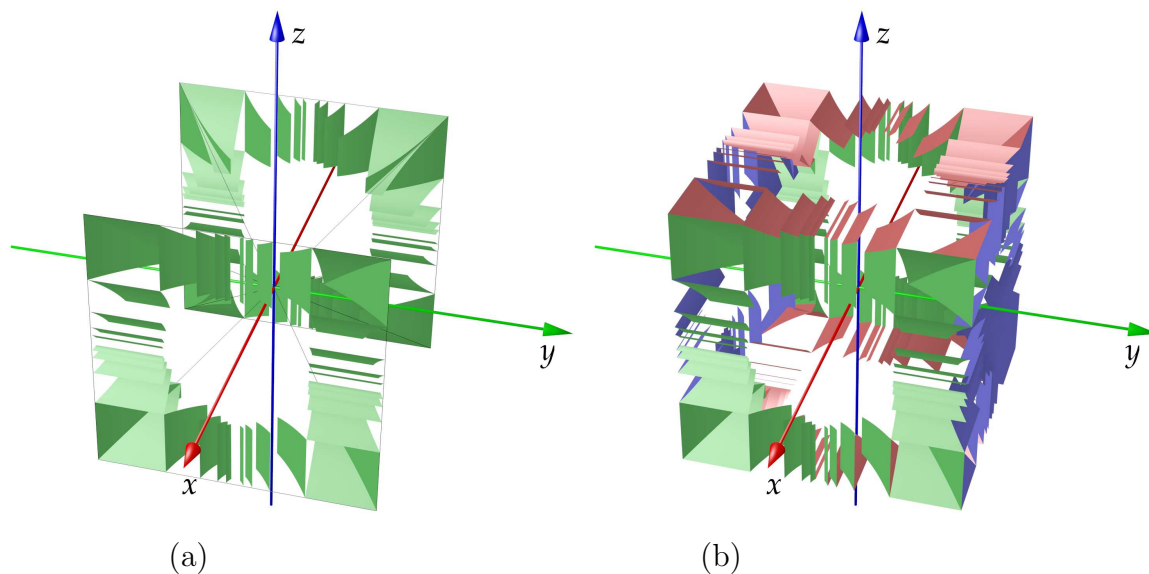


Figure 14: A body invisible in the direction along the x -axis (a) and a body invisible in 3 directions (b)

directions has an infinite number of connected components. We wonder if the increased complexity of the shape is the cost one should pay for the increased number of directions, or whether it is just an artefact of the particular constructions.

These problems are easy to understand, and the existing results can be explained by using only basic school math. However, there are no *tools* or *techniques* for constructing invisible bodies, and this makes the subject even more exciting.

Acknowledgements

This work was partly supported by the Center for Research and Development in Mathematics and Applications (CIDMA) from the "Fundação para a Ciência e a Tecnologia" (FCT), cofinanced by the European Community Fund FEDER/POCTI, and by the FCT research project PTDC/MAT/113470/2009.

References

- [1] A. Aleksenko and A. Plakhov. *Bodies of zero resistance and bodies invisible in one direction*. *Nonlinearity* **22**, 1247-1258 (2009).

- [2] D. Bucur and G. Buttazzo, *Variational Methods in Shape Optimization Problems*. Birkhäuser (2005).
- [3] G. Buttazzo and B. Kawohl. *On Newton's problem of minimal resistance*. Math. Intell. **15**, 7-12 (1993).
- [4] M. Comte and T. Lachand-Robert. *Newton's problem of the body of minimal resistance under a single-impact assumption*. Calc. Var. Partial Differ. Equ. **12**, 173-211 (2001).
- [5] T. Lachand-Robert and E. Oudet. *Minimizing within convex bodies using a convex hull method*. SIAM J. Optim. **16**, 368–379 (2006).
- [6] T. Lachand-Robert and M. A. Peletier. *Newton's problem of the body of minimal resistance in the class of convex developable functions*. Math. Nachr. **226**, 153-176 (2001).
- [7] I. Newton, *Philosophiae naturalis principia mathematica*. 1687.
- [8] A Plakhov. *Scattering in billiards and problems of Newtonian aerodynamics*. Russ. Math. Surv. **64**, 873938 (2009).
- [9] A Plakhov and A Aleksenko. *The problem of the body of revolution of minimal resistance*. ESAIM Control Optim. Calc. Var. **16**, 206-220 (2010).
- [10] A Plakhov and V Roshchina. *Invisibility in billiards*. Nonlinearity **24**, 847–854 (2011).
- [11] <http://en.wikipedia.org/wiki/Invisibility>
- [12] <http://de.wikipedia.org/wiki/Unsichtbarkeit>